

Diamond as a magnetic field calibration probe

J Maes¹, K Iakoubovskii², M Hayne¹, A Stesmans² and V V Moshchalkov¹

¹ Laboratorium voor Vaste-Stoffysica en Magnetisme, K U Leuven, Celestijnenlaan 200 D, B-3001 Leuven, Belgium

² Laboratorium voor Halfgeleiderfysica, K U Leuven, Celestijnenlaan 200 D, B-3001 Leuven, Belgium

Received 19 January 2004

Published 17 March 2004

Online at stacks.iop.org/JPhysD/37/1102 (DOI: 10.1088/0022-3727/37/7/024)

Abstract

An optical method is proposed for the calibration of pulsed magnetic fields using photoluminescence from synthetic diamond. Generally, the pulsed magnetic field profile is reconstructed by measuring the pick-up voltage in a small coil with an effective area that needs to be known accurately. A useful method to calibrate this area is presented using the 1.4040 eV optical transition at the 1.4 eV Ni-related centre in diamond. The field value is calculated from the Zeeman splitting of the optical lines using the g -factor previously characterized by electron spin resonance. Numerous advantages of the method presented are discussed.

1. Introduction

1.1. Some aspects of magnetic field calibration

A broad range of applications of magnetic measurements underlines the importance of absolute calibration of the magnetic field strength B (Herlach and Miura 2003). Several accurate and reliable procedures are known for calibration of low-field ($B < 15$ T) dc magnets, such as the magnetic phase transition and the magnetic resonance marker methods. In the first method, a specific magnetic material is placed in the magnet to be calibrated, and the time derivative of magnetization, dM/dt , is monitored. At certain magnetic field values, dM/dt shows discontinuities which can be used for field calibration. The marker method utilizes magnetic level splitting (the Zeeman effect) in a certain magnetic nucleus (the nuclear magnetic resonance probe) or in an electronic defect centre in a solid [the electron spin resonance (ESR) g -marker (Stesmans and Van Gorp 1989)]. It relies on the knowledge of the spectroscopic splitting factor g and the ability to measure the resonance frequency. The latter is generally not a limiting factor. So, provided that g is accurately known, a high accuracy calibration can be attained.

In the high-field ($B \sim 60$ T) pulsed magnets, a capacitor discharge into a conductive solenoid results in the production of a millisecond-long magnetic field pulse exhibiting a damped sine shape. The field intensity in the coil can be easily monitored using a small metallic (copper wire) pick-up

coil, but the absolute field calibration is not straightforward. Generally, an external time-dependent magnetic field $B(t)$ applied parallel to the coil axis induces a voltage over the coil $V(t) = -S_{\text{eff}} \times dB(t)/dt$. Here, S_{eff} is the effective coil area, which takes into account the coil geometry, number of windings and the (small) field inhomogeneity. This parameter is difficult to calculate accurately, and thus should rather be determined from an independent measurement. Unfortunately, both the phase transition and the marker method mentioned above are hardly applicable for this purpose: phase transitions may appear too inertial, while the marker methods would require construction of a complex pulse-field resonance spectrometer solely for the purpose of calibration. Conventionally, such a spectrometer would require a microwave waveguide to be fed into the high-field magnet core, which poses electromagnetic and engineering problem of prohibitive nature. However, most high-field magnets easily allow access via an optical waveguide, thus suggesting following field calibration procedure: a substance should be selected containing a specific paramagnetic centre, that should exhibit an efficient optical transition(s) between an excited state and the ground state. Photoluminescence (PL) transitions should be preferred over optical absorption because of the inherent higher detection sensitivity and easier optical access, i.e. no need to pass light through the sample, meaning that reflection-style geometry with one-way optical access is sufficient and with milder requirements as to the

sample transparency. The magnetic field splitting of the ground and excited states should be described by a simple spin Hamiltonian H , preferably of the form $H = g\mu BS$, where μ is Bohr magneton, and S the z -component of the electron spin. Provided that the g -factors pertaining to the ground and excited states (g_{gr} and g_{ex} , respectively) are accurately calibrated with one of the dc calibration methods described earlier, the pulsed field value can be found from the splitting of the PL transitions as

$$\Delta E = \mu B |S_{gr}g_{gr} - S_{ex}g_{ex}| \quad (1)$$

The PL measurements can be easily performed with a simple, inexpensive table-top PL spectrometer. Obviously, however, the major difficulty lies in the availability of a proper calibration substance, which should satisfy at least three basic criteria:

- (1) It should be mechanically and chemically stable.
- (2) It should exhibit an intense and sharp-line PL, easily detectable with high spectral resolution during a short (ms) magnetic field pulse.
- (3) It should have significantly different and measurable values of $S_{gr}g_{gr}$ and $S_{ex}g_{ex}$.

In this respect, we note that efficient electrical dipole allowed transitions usually require $S_{gr} = S_{ex}$. Furthermore, it appears that both g_{gr} and g_{ex} of many defects in solids are close to the free electron value $g_e = 2.002\,319$, thus resulting in a rather small magnetic field splitting (see equation (1)), and that the desired deviations of g_{gr} and g_{ex} from g_e mostly originate from spin-orbit coupling, which strongly increases with the atomic number.

Considering the above criteria and remarks, a most obvious calibration standard for high pulsed magnetic fields would appear a transition metal ion (large spin-orbit coupling) related centre in a transparent, non-magnetic solid, such as Cr^{3+} in Al_2O_3 (ruby). Indeed, ruby is a rather stable technological material, exhibiting very efficient (laser) PL transitions at ~ 1.79 eV. Unfortunately, the ground state of the Cr^{3+} impurity is a spin triplet exhibiting strong spin-spin interaction (~ 0.2 T). This results in a non-linear spin Hamiltonian thus complicating the analysis of the splitting pattern. Therefore, in this paper we propose an alternative standard for the calibration of pulsed magnetic fields, namely the 1.4 eV Ni-related centre in synthetic diamond, which we show is highly suitable for that purpose.

1.2. Electronic properties of the 1.4 eV Ni-related centre in diamond

Nickel is one of the most popular catalysts for the growth of diamond using the high-pressure high-temperature (HPHT) technique. It has been found that during the synthesis, dispersed Ni atoms are incorporated exclusively in the $\{111\}$ growth sectors of diamond, resulting in a number of optical centres. We shall focus here on the sharp lines at 1.4040 and 1.4012 eV, which are the dominant features of the so-called 1.4 eV Ni-related centre. The lowest ground state of this centre gr_1 (see figure 1) has been characterized by ESR (Isoya *et al* 1990). It was attributed to an interstitial Ni^+ related $S = \frac{1}{2}$ centre of trigonal symmetry. The angular dependence

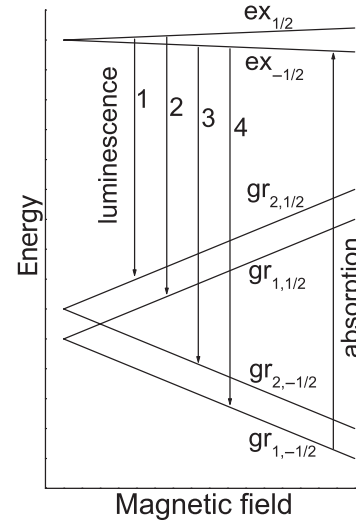


Figure 1. Schematic diagram of some of the optical transitions at the 1.4 eV centre in diamond at helium temperatures with the magnetic field applied along the $\langle 111 \rangle$ crystal axis. The ground and excited states are labelled as $gr_{1,\pm 1/2}$, $gr_{2,\pm 1/2}$ and $ex_{\pm 1/2}$, respectively, where $\pm 1/2$ is the z -component of the electron spin.

of ESR lines could be accurately simulated with a simple spin Hamiltonian $H = g\mu BS$. The principal components of the g matrix were deduced as $g_{1gr1} = 2.329(5)$, $g_{2gr1} = g_{3gr1} = 0$ (≤ 0.1), with g_{1gr1} aligned to the $[111]$ crystal axis.

The optical transitions of this 1.4 eV centre have been characterized by optical absorption and luminescence with (Mason *et al* 1999, Nazare *et al* 1991) and without (Collins 1989) an applied magnetic field. Those measurements revealed that the 1.4040 and 1.4012 eV lines (energies at zero magnetic field) originate from transition between three Kramers doublets (degenerate only by spin $S = \frac{1}{2}$), one in the excited state ($ex_{\pm 1/2}$) and two, separated by 2.8 meV, in the ground state ($gr_{1,\pm 1/2}$ and $gr_{2,\pm 1/2}$ in figure 1). All transitions are further split into narrow-spaced (~ 0.17 meV) multiplets (not shown in figure 1), which were assigned to different Ni isotopes for a defect involving one Ni atom. The trigonal symmetry inferred from ESR (Isoya *et al* 1990) was confirmed by uniaxial stress PL measurements (Nazare *et al* 1991), and, moreover, an unusual orientational polarization of the 1.4 eV centre was revealed. Normally, a trigonal centre in the diamond lattice has four equivalent orientations. Yet, it is found that within a single $\{111\}$ growth sector of an HPHT diamond, the 1.4 eV centres are aligned exclusively to the $[111]$, but not to the $[\bar{1}\bar{1}\bar{1}]$ or $[\bar{1}\bar{1}1]$ crystal axes (Collins 1989).

While only the lowest ground state could be characterized by ESR (Isoya *et al* 1990), the g -factors for all three Kramers doublets have been assessed by magneto-optical measurements (Mason *et al* 1999, Nazare *et al* 1991). Unfortunately, only relatively low (≤ 6 T) dc magnetic fields were applied in those studies, and as a consequence, the splitting was poorly resolved, resulting in low accuracy. The g -values for the excited state were deduced as $g_{1ex} = 0$ (≤ 0.1), $g_{2ex} = g_{3ex} = 2.4(1)$. The g_1 value of the higher lying ground state g_{1gr2} was estimated to be in the range 1.6–2 (Mason *et al* 1999, Nazare *et al* 1991). In this work, application of higher magnetic fields (≤ 49 T) allowed more accurate determination of the g_{1ex} and

In order to separate a single $\{111\}$ growth sector, a thin slice was laser cut from a $\{111\}$ facet $[(1\bar{1}1)$ facet in figure 4(a)], normal to the surface, as indicated by the dashed line in figure 4(b). The slice was then polished and mounted into the magnet with the probe fibres and the magnetic field normal to the (111) sample surface (see figure 2). This sample preparation procedure was chosen to simplify the PL spectra and to increase the magnetic splitting (see equation (1)). Indeed, the results summarized in section 1.2 indicate that the 1.4 eV centres are aligned to the $[111]$ direction in a single (111) growth sector, and thus only the g_1 , but not g_2 and g_3 , components of the \mathbf{g} matrices determines the magnetic splitting. Moreover, for the $[111]$ oriented magnetic field $g_{1ex} = 0$ and g_{1gr1} reaches its maximum value (2.329), thus maximizing ΔE (see equation (1)).

PL measurements were performed at 4.2 K using 2.41 eV laser excitation from an argon-ion laser. Typical results are summarized in figure 5, where part (a) shows typical PL spectra. The derived peak positions as a function of magnetic field are plotted in figure 5(b), and the integrated intensities of lines 1 and 4, as well as of the total PL spectrum, are shown in figure 5(c). Lines 2 and 3 were only partially resolved for most magnetic field values assessed and therefore, to provide reliable data, a half-sum of their intensities is plotted in figure 5(c). The triangular-like lineshape of the signals shown in figure 5(a) is caused by the unresolved Ni isotopic splitting of each line (the major Ni isotopes have natural abundances of 68.27% for ^{58}Ni , 26.1% for ^{60}Ni and 3.59% for ^{62}Ni). Calibration of the magnetic field was achieved by matching the slopes for lines 2 and 4 (figure 5(b)) to the values $S_{gr1}g_{1gr1}\mu_B$, where $g_{1gr1} = 2.329$ as previously deduced by ESR (Isoya *et al* 1990) and $S_{gr1} = \pm\frac{1}{2}$. Concomitantly, the g value for the second ground state (lines 1 and 3) was determined here as $g_{1gr2} = 1.93(2)$. It is important to note that this calibration relies on the assumption $g_{1ex} = 0$, which will be justified in section 4.

The calibration procedure described requires detection of the magnetic field splitting between lines 2 and 4, for which purpose a particular laser-cut slice was prepared in this study. However, measurements performed before the sample was cut revealed that although the splitting pattern from the whole diamond crystal is more complex than that from a (111) slice, lines 2 and 4 could still be clearly separated. Therefore, a whole as-grown HPHT crystal can be used for the proposed calibration method. Moreover, the 1.4 eV lines are sufficiently sharp even at nitrogen temperatures (linewidth ~ 0.8 meV at 77 K), and thus the calibration procedure does not even require a He cryostat.

4. Analysis

The proposed magneto-optical marker calibration method relies on the knowledge of the values g_{1gr1} and g_{1ex} (see equation (1)). While g_{1gr1} for the 1.4 eV centre was previously accurately determined by ESR as 2.329(5), only a rough estimate was available for g_{1ex} . In this work, application of low temperatures and high magnetic fields allowed us to increase the accuracy of the g_{1ex} value by an order of magnitude. This is attained starting from the analysis of figure 5(c), where, clearly, two regions, 0–25 and 25–49 T, can be distinguished: a key observation is that the line intensities

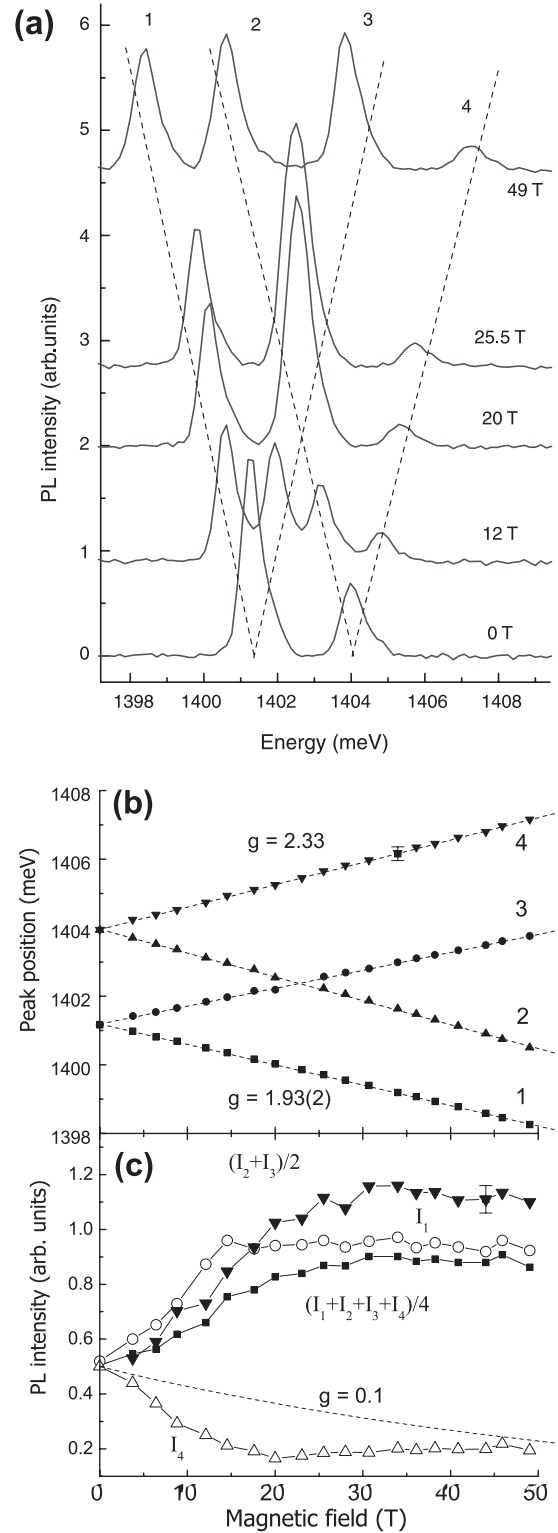


Figure 5. Magneto-PL data obtained at 4.2 K under 2.41 eV laser excitation with the pulsed magnetic field applied along a (111) crystal axis: (a) PL spectra for selected field values; dashed lines indicate the splitting behaviour as a function of magnetic field. (b) Peak positions; dashed lines present linear fits to the data based on the Zeeman splitting $g\mu_B S_Z$. (c) Intensities of the observed lines and some combinations as a function of the magnetic field. Solid lines in (c) are guides for the eye, while the dashed line depicts the expected thermalization behaviour of the PL intensity for $g_{1ex} = 0.1$ (see text for details).

versus magnetic field remain constant in the second region. Indeed, the magnetic splitting in the excited state of the 1.4 eV centre may cause electron thermalization thus resulting in a (slight) intensity increase for lines 3 and 4, which would result in a corresponding intensity decrease for lines 1 and 2 (see figure 1). The expected effect on the intensity of lines 1 and 2 of such a thermalization behaviour, corresponding to the magnetic splitting with $g_{1ex} = 0.1$ (upper limit given by Mason *et al* 1999), is simulated and presented by the dashed line in figure 5(c). The experimental data, however, show no significant intensity variation in the field range 25–49 T. This suggests that the splitting in the excited state is rather small, from where it is inferred that $g_{1ex} < 0.01$. The latter improved estimate justifies, within the current accuracy, the assumption $g_{1ex} = 0$ made in the calibration procedure outlined in section 3.

In the first region (0–25 T) in figure 5(c), the intensities of the lines 1 and (2 + 3) increase, but the intensity of the line 4 decreases. This behaviour can be partially explained by self-absorption, as described below (see figure 1): at the low temperature of our experiment (4.2 K) only the lowest ground state gr_1 is populated. Therefore, at zero magnetic field, PL originating from transitions $ex_{\pm 1/2} \rightarrow gr_{1,\pm 1/2}$ (PL lines 2 and 4), but not $ex_{\pm 1/2} \rightarrow gr_{2,\pm 1/2}$ (PL lines 1 and 3), is partially absorbed via transitions $gr_{1,\pm 1/2} \rightarrow ex_{\pm 1/2}$. Note that optical dipole transitions $gr_{1,+1/2} \rightarrow ex_{-1/2}$ (or $gr_{1,-1/2} \rightarrow ex_{+1/2}$) are spin forbidden and thus can be neglected here. Increasing magnetic field results in the splitting of the level gr_1 into $gr_{1,+1/2}$ and $gr_{1,-1/2}$. Consequently, electrons thermalize into the level $gr_{1,-1/2}$. As a result, the absorption transition $gr_{1,-1/2} \rightarrow ex_{-1/2}$ is enhanced (and is drawn in figure 1) and that of $gr_{1,+1/2} \rightarrow ex_{+1/2}$ is quenched. Correspondingly, the PL transition 4 (2) becomes more (less) self-absorbed. Note, that this simple model would naturally explain the intensity decrease of PL line 4 and increase of line 2 in figure 5(c), but not the intensity variations of lines 1 and 3. The origin of the latter variations is yet unclear and requires further investigation.

5. Conclusion

In conclusion, we have developed a simple method for calibration of pulsed magnetic fields. The field is continuously measured by a voltage across a small pick-up coil inserted into the magnet. This voltage is calibrated utilizing the Zeeman splitting of the 1.4040 eV PL transition at the 1.4 eV Ni-related centre in synthetic diamond, the splitting being measured with magnetic field along a $\langle 111 \rangle$ crystal axis. Application of high magnetic fields (49 T) along a $[111]$ direction and of low temperatures (4.2 K) in this study allowed accurate determination of the g values at the 1.4 eV centre: $g_{1gr2} = 1.93(2)$ for the second, higher-lying ground state, and $g_{1ex} < 0.01$ for the excited state.

Acknowledgments

The authors are grateful to H Kanda (NIMS, Japan), I Kiflawi (Reading University, UK) and A Taylor (DTC Research Centre) for preparation and provision of the diamond sample. KI acknowledges illuminating discussions with Prof. J M Baker. This work has been supported by the FWO-Vlaanderen, the Belgian IUAP programmes, and the VIS 00/001 project of the K U Leuven and the SBO-project 30219 of the IWT-Vlaanderen.

References

- Collins A T 1989 *J Phys.: Condens. Matter* **1** 439
- Herlach F and Miura N 2003 *High Magnetic Fields: Science and Technology* (Singapore: World Scientific) ISBN 9810246986
- Isoya J, Kanda H and Uchida Y 1990 *Phys. Rev. B* **42** 9843
- Mason P W, Ham F S and Watkins G D 1999 *Phys. Rev. B* **60** 5417
- Nazare M H, Neves A J and Davies G 1991 *Phys. Rev. B* **43** 14196
- Rosseeel K, Lagutin A, Herlach F, Boon W, Bruynseraede Y and Van Humbeeck J 2002 *IEEE Trans. Appl. Supercond.* **12** 707
- Stesmans A and Van Gorp G 1989 *Rev. Sci. Instrum.* **60** 2949
- Vanacken J 2001 *Physica B* **294–295** 591